AG

by Raja Annamalai

Submission date: 14-Sep-2022 12:34AM (UTC-0700)
Submission ID: 1899502499
File name: Dr._KK_-_Revised_Ag_NPs_Manuscript_-_Without_Author.docx (1.95M)
Word count: 3182
Character count: 18387

Synthesis and antimicrobial activity of silver nanoparticles: Incorporated *couroupita guianensis* flower petal extract for biomedical applications

Abstract

Recently, numerous plant-based synthesis techniques have been used to develop metal nanoparticles. The current study uses the medicinal plant extract of *couroupita guianensis* (CG) petals to create biogenic silver nanoparticles in an environmentally friendly manner. Different techniques, including ultraviolet-visible spectroscopy (UV-vis), Fourier Transformation Infrared spectroscopy (FTIR), X-ray diffraction (XRD), and Dynamic Light Scattering (DLS) analysis, are used to evaluate synthesized silver nanoparticles. From the XRD results confirm the emergence of nanosilver crystalline arrangement with the characteristic peaks at the glancing angles of 38.04°, 44.22°, 64.40°, and 77.37°. UV-vis spectroscopy displays the spectral absorption at λ_{max} = 282 nm and shows the formation of silver nanoparticles. Images of produced Ag NPs taken with a scanning electron microscope (SEM) show the creation of flower-shaped particles. The functional behavior of flavones, triterpenoids, and polyphenols belonging to *couroupita guianensis* has been observed by ensuring their selective absorptions in FTIR spectral analysis silver nanoparticles had a substantial antibacterial effect on Gram-positive (*B. subtilis*) and Gram-negative (*Escherichia coli*) bacteria in general. It is found to become effective when symbiotic with the extract of *couroupita guianensis* flower petals for enhancing their antibacterial properties. This composite product gives a new and cost-effective formulation with more therapeutic possibilities. The observed results wide open the avenues of research possibilities with a lot of future scopes. The photocatalytic degradation efficiency of CG-Ag NPs on methylene blue (MB) dye was evaluated under visible light irradiation and produced indications of the synthesized material for photocatalytic applications.

Keywords: *Couroupita guianensis flower* petals, silver nanoparticles, SEM analysis, X-ray, DSL analysis, antimicrobial activity, and photocatalytic activity.

1. Introduction

Medicinal plants are special elements known for their therapeutical scope and render long-time remedies for several human diseases. It is mainly because of the healing value of their components used as a raw material in modern medicine. The *couroupita guianensis* (CG) is a tree and its parts are familiar components used for medicinal purposes. Particularly, its chemical ingredients are responsible for various pharmacological and therapeutic properties. The study used to explore the characteristic features of *couroupita guianensis* is essentially required to prove its potential in clinical applications. Under the discipline of materials science, the nanomaterial is a fast-growing area that renders various types of materials find application in a wide variety of fields including medical, chemical, catalytic, mechanical, electronic, and environmental industries [1-4]. Various synthesis routes are available to produce nanomaterials employing physical, chemical, and biological methods [5-7]. Nanomaterial synthesis also causes adverse effects producing environmental (or) pollution-related issues. Nanotechnology also supports rectifying these pollution-related issues with nanoscale materials of various types. The application potential of nanomaterials is wide in clinical issues in the field of biomedical. Silver nanoparticle (Ag NPs) is one of the elements proven their biological characteristic for many clinical issues. The use of biological sources such as bacteria, fungi, algae, and plants in the green production of silver nanoparticles is one of the most promising ways. Previous studies have shown that leaf [8], flower buds [9], fruit [10], stem [11], root [12], and flower extracts are inadequate biological approaches for producing AgNPs [13-18]. It is generally suggested that the synthesis of silver nanoparticles using plant materials is a promising, profitable method easy to scale. In the present work, the extract of a medical plant from the family of Lecythidaceae namely, Couroupita guianensis is symbiotic with the silver nanoparticle for biomedical applications. Fig. 1 displays the floral flakes of c*ouroupita guianensis* colored with yellow, red, and pink in stunning scenic color. Widely used medicinal plants in India have indicated a broad spectrum of antimicrobial and antifungal activities. The flowers of couroupita guianensis have signified sufficient antioxidant activity. The phenolic compound of petals is active in the treatment of renal and stomach problems and has anti-inflammatory effects [19].

The biological function of flavonoids, in addition to their antioxidants, includes protection against allergies, inflammation, platelet aggregation, microorganisms, ulcerates, hematoxylin, viruses, and tumors. Isatin is one of the effective components of the medicinal plant *couroupita guianensis*, known well for its cytotoxic action contrary to certain lines of tumor cells and it is found to be a potential source of new chemotherapy agents. It is used to treat hypertension, tumors, pain, inflammatory processes, cold, stomachache (norovirus), skin diseases, malaria (rotavirus), wounds and toothache [20]. *E. coli* and *Bacillus subtilis* strains, as well as the effect of AgNPs on the growth of both bacterial, it was a very effective inhibitor of *E. coli* and *B. subtilis* growth [21]. The present study aimed to synthesize silver nanoparticles from aqueous extracts of petals of the medicinal plant couroupita guianensis. The characterization has been summed up using various techniques used for assessing their size, morphological characteristics, and antimicrobial activity. In the current work, we have chosen *Couroupita guianensis* dopant for silver nanoparticles (AgNPs) to improve photocatalytic performance. Antibacterial, optical, thermal, and catalytic characteristics of silver NPs are all controlled by their size and form. Ag is an excellent conductor with a decent bandgap and optical properties. The addition of CG to AgNPs will affect their antibacterial properties as well as the rate of electron-hole pair recombination. The report discusses visible-light-induced improved photocatalytic degradation utilizing CG doped AgNPs catalyst produced using the sol-gel method [22, 23].

2. Materials and procedure

2.1 Plant material sampling and identification

Raw chemicals of analytical grade (AR) with a purity of ≥ 99% of silver nitrate have been purchased from E-Merk life science private limited, Mumbai, India. The fresh and healthy petals of the *couroupita guianensis* flowers were collected around the fertile land located in Salem, Tamil Nadu, India. Following schematic procedures like washing, and sterilizing used to remove impurities from the fresh floral flakes facilitates the preparation of the flower petals suitable to collect the extract.

Fig. 1. Couroupita guianensis flower petal

2.2 Preparation of flower petal extract

The washed floral flakes were dried and 5 gm weighted flakes were immersed in 50 ml distilled water taken in100 ml beaker and boiled for 20 minutes. After boiling, the extract was cooled and filtered using a Whatman No 1 filter paper and filter paper (size 0.4 m) in a sequence to create a final extract, which was then stored at 4 °C.

2.3 Silver nanoparticle synthesis

In a conical flask, 50 ml of 1 mM aqueous silver nitrate was combined with 5 ml of floral flake extract. The solution mixture has been stirred vigorously in a magnetic stirrer for 15 minutes. The process lasts for 30 minutes and until the silver ions are reduced to silver particles at room temperature. The hue of the reaction mixture shifted from blue green to brown after 30 minutes, according to the researchers. It shows that the UV-visible spectrophotometer can guarantee the reduction of silver ions into AgNPs.

3. Results and Discussion

3.1 X-ray diffraction analysis

Observed X-ray powder diffraction (XRD) results recorded the details of the crystal lattice and the structure of the synthesized AgNPs as given in Fig. 2. The X-ray diffractogram evident the emergence of diffraction peaks at the glancing angles (2θ) 38.04°, 44.22°, 64.40°, and 77.37° which parallel to the planes of the cubic structures of silver nanoparticles (111), (200), (220), and (311). As reported elsewhere [24], the observed peaks and their glancing angles are agreed well with the previous observations as evident in the emergence of crystalline silver nanoparticles with cubic structures. The result of XRD agrees with earlier plant-based synthetic reports [25]. The Scherrer equation was used to calculate the average crystallite size of produced AgNPs, and the average crystallite size was determined to be 34 nm (Table 1). The existence of prominent crystalline peaks without any more impurity peaks has proven the emergence of pure crystalline silver nanoparticles.

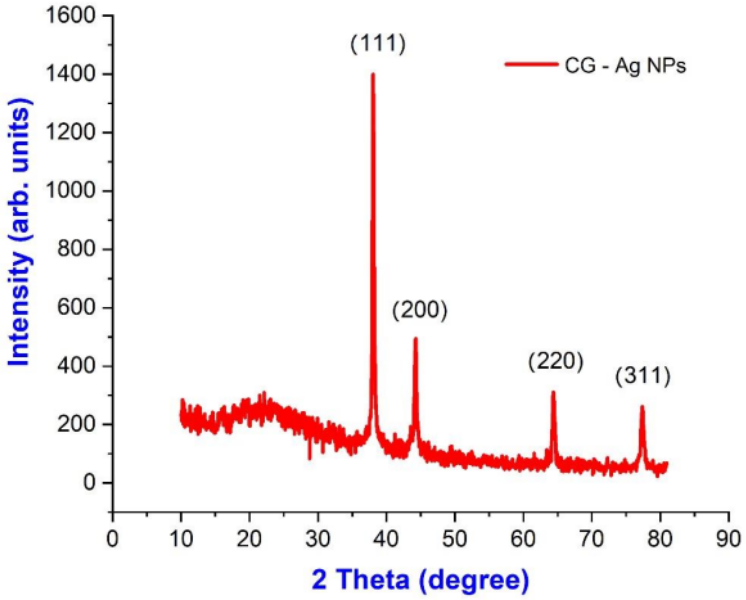

Fig. 2. X-ray diffraction spectrum of *Couroupita guianensis* flower petal extract synthesized AgNPs

Table 1. Crystallite size estimated from the XRD of AgNPs

S. No	Pos. [2° degree]	FWHM. [2° degree]	d-spacing [Å]	Crystallite size
1	38.0421	0.2460	2.36545	35.69
2	44.2284	0.2952	2.04789	30.35
3	64.4014	0.2460	1.44672	39.88
4	77.3702	0.3444	1.23342	30.88

3.2 UV-visible spectroscopy analysis

UV spectrum obtained from the synthesized sample of silver nanoparticles with the incorporation of petal extract of couroupita guianensis is represented in Fig. 3. It reveals the traces of silver ions as evident of bio-reduction from silver oxide. It also could be visually observed with color variations in the solution combination from light blue to dusky brown after 30 minutes of the reaction process. Observed changes in solution color may be because of bilateral electromagnetic fields generated by coordinated oscillations of free electro heads in surface plasmon resonance [26]. Spectral absorption of AgNPs depends mainly on the particle size, medium, and chemical environment. Hence, UV-vis spectroscopy analysis facilitates the identification of the reduction of silver ions while scanning in the wavelength range of 200 to 600 nm. It is known from the standards data that characteristic absorption of silver nanoparticles is found to be existing in the range around 212 and 281 nm as shown in Fig. 3.

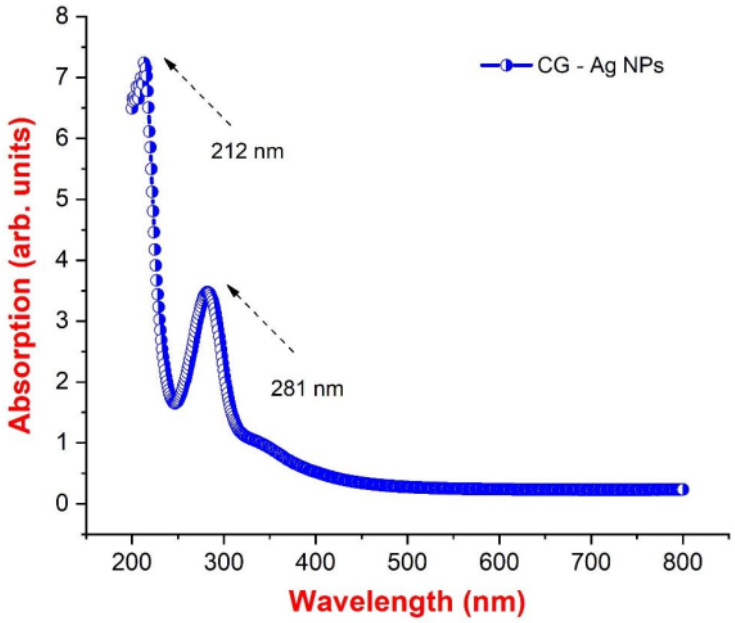

Fig. 3. UV visible spectrum of synthesized AgNPs using flower petal extracts of *Couroupita guianensis*.

3.3 FTIR analysis

Biosynthesis silver particles on the nanoscale are usually stabilized by phytochemical compounds through molecular interactions with metal surfaces. FTIR analysis can be used to explore the nature of the molecular interaction and its functionalities as reported in the literature based on the functional group reference peaks. This analysis also could reveal the interaction between silver nitrate and boilers present in the flower extract from couroupita genesis. Fig. 4 shows the observed FTIR spectrum of the sample showing the peaks at wavenumbers 3939 cm^{-1}, 3336 cm^{-1}, 3018 cm^{-1}, 2765 cm^{-1}, 2039 cm^{-1}, 1475 cm^{-1}, 969 cm^{-1}. All characteristic peaks evident the existence of silver nanoparticles from biosynthesis and the peaks corresponding to the molecules that can be involved in the synthesis and stabilization of silver nanoparticles. The absorption bands at 3939 cm^{-1} parallel to the vibrations of O-H between the molecules (amines of phenolic and alcoholic compounds). The peaks in rang 3336 cm^{-1} are among the flavones, triterpenoids, and

polyphenols. Thus, the interaction between the ions of metals and the group of amides in the flake extract of couroupita genesis is involved in the synthesis and stabilization (capping) of the nanosilver formation, as previously described [26]. Peaks located at wavenumbers 3018 cm^{-1} and 2765 cm^{-1} represented groups of phenols, amines, and the presence of stretching alkanes. The absorption bands at 2765 cm^{-1} and 2039 cm^{-1} on the other hand, correspond to asymmetric and symmetric stretching of -CH_2 and -CH, respectively. C-H aliphatic vibrations may be responsible for the absorption band at 2039 cm^{-1}. The peak at 1475 cm^{-1} investigates the vibrations C=O of -COOH. The carbon-carbon double bond C=C is responsible for the bands at 1475 cm^{-1}. The C-N tensile aromatic amines are represented by the strong peaks at 1074 cm^{-1} and 969 cm^{-1}. The presence of amino (-N-H) functional groups accounts for the absorbance at 824 cm^{-1}. The 767 cm^{-1} and 668 cm^{-1} characteristic bands were identical to the alkane's groups discovered in the plant extract, which could alter nanoparticle production.

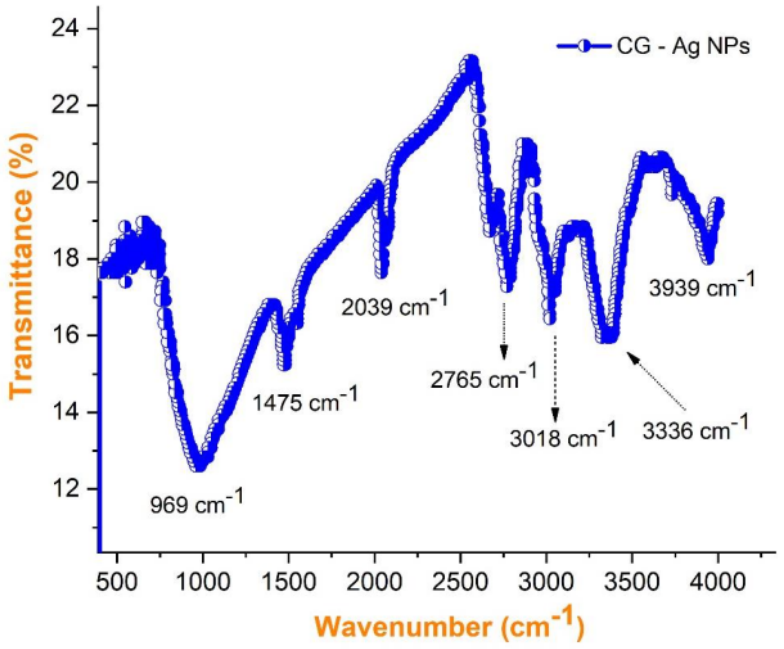

Fig. 4. FTIR spectra of synthesized AgNPs using flower petal extracts of *Couroupita guianensis*.

3.4 Scanning electron microscope (SEM) analysis & DLS analysis

Using an extract from the flower petals of *Couroupita guianensis*, the surface morphology images investigate the size and shape of the produced silver nanoparticles. The SEM characteristics of the prepared nanoparticles Ag are found in Fig. 5(a-b). The SEM illustration exhibited a sponge-like structure of nanoparticles ranging up to 20 nm. The result of hydrodynamic size estimation of silver nanoparticles employed using DLS analysis is given in Fig. 5(c). It shows the average particle size distribution of silver nanoparticles (diameter = 3.2 nm and Standard Deviation = 1.9 μm) is signified within the range of 3.2 nm as listed in Table 2. It ensures the screening of small particles by larger phytochemicals of couroupita genesis attached to the surface of AgNPs [25].

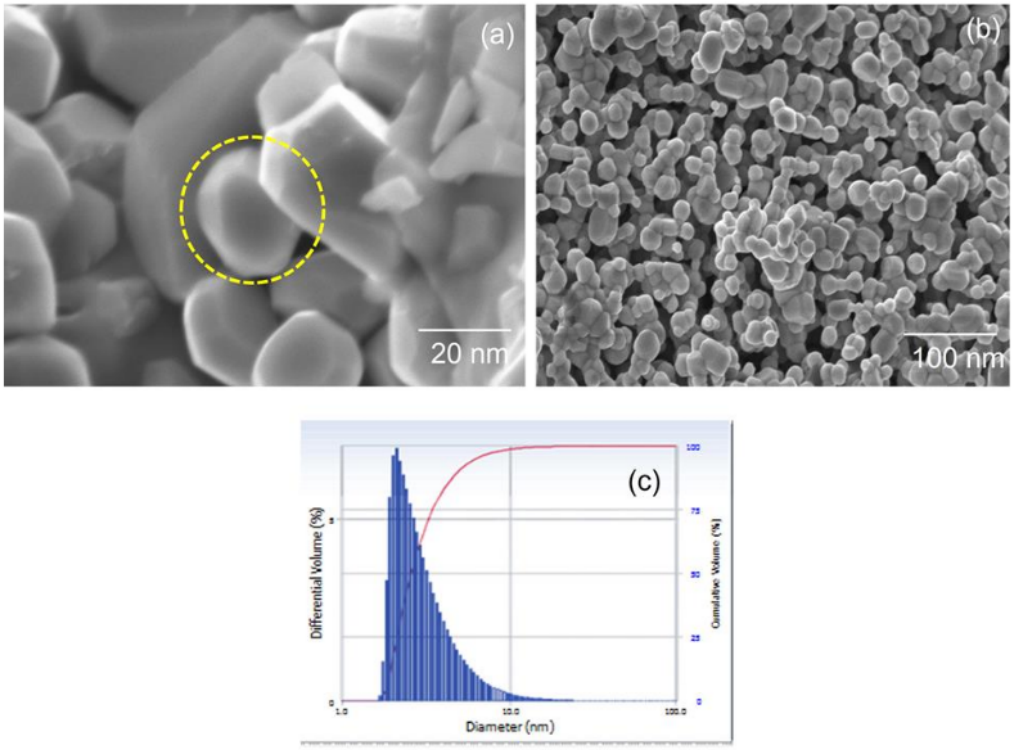

Fig. 5(a-b). Scanning electron microscopy images of silver nanosponges synthesized from *Couroupita guianensis* flower petal extracts; (c) Dynamic Light Scattering of AgNPs using flower petal extracts of *Couroupita guianensis*.

Table 2. Dynamic light scattering (DLS) of AgNPs synthesized from flower petal extract of *Couroupita guianensis* indicating the average particle size and distribution of nanoparticles

S. No	Peak	Diameter (nm)	Std. Dev.
1	1	3.2	1.9
2	2	0	0.0
3	3	0	0.0
4	4	0	0.0
5	5	0	0.0
Average		3.2	1.9

3.5 Antibacterial activities

Although there are numerous analytical procedures for evaluating AgNPs' antibacterial activity, the standard and the most susceptible process is the plate diffusion method. Observed results of antibacterial activities of flake extract containing silver nanoparticles against Gram-positive (*B. Sublimus*) and Gram-negative (*E. Coli*) are shown in Fig. 6 with the zone of inhibition. AgNPs have strong inhibitory activity against Gram-positive bacterial species. For Bacillus subtilis (Table 3) a maximum inhibition zone is observed to be 16 mm. AgNPs have shown higher bactericidal activity in Bacillus subtilis compared to the negative Escherichia coli Gram. As reported in the literature, different mechanisms for the antibacterial activity of similar compounds from the flowers of croupier guianensis. The major bacteriological activity of the floral extract against bacterial species is mainly because of the existence of numerous antibacterial compounds, such as flavonoids, phenols, flavor compounds, isatin, and indiglumin. As reported in the literature, the antibacterial activity of identical extracts is possible from combinations of the croupier guianensis [27, 28]. The plants containing phenolic compounds are known well for their bio-related activities, such as antibacterial, fungicide, antibacterial, anti-mutagen, and anti-inflammatory drugs, which have been assigned to their hydroxyl groups (-OH) [29]. Many aliphatic hydrocarbons, quercetin, and stigmainol from extracts of floral flakes, as mentioned earlier, also support antibacterial activity. Quinine is the main phenolic compound of a flower which leads to the loss and deactivation of its functions. In antibacterial activity, the most common targets are surface adhesion, cellular wall polypeptides, and membrane-related enzymes. Flazonide is known for the restriction of *B. subtilis* and *Escherichia* in respect of the class of flavonoids *E. Coli* by binding

with ATP to the party. Induced DNA also increases the melting capacity of bacterial membranes and the loss of potential membranes. The antimicrobial action was responsible for the multiple and exhibited effects of the compounds in floral extracts [30-32]. The combined effect of a floral mixture and nano form can be explained by the increased proportion of surface to volume of the nanoparticles, which provides the largest contact area with bacteria [33-36].

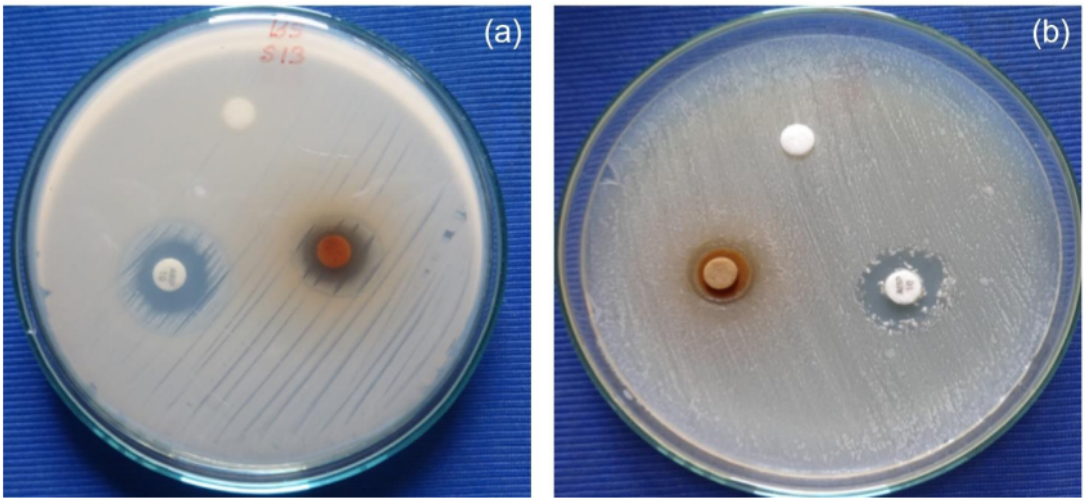

Fig. 6. Antibacterial activity of AgNPs against Gram Positive (*Bacillus subtilis*) and Gram Negative (*Escherichia Coli*) stains.

Table. 3. Zone of Inhibition of AgNPs against Gram - positive and Gram - negative bacteria strain

S. No.	Bacteria	Zone of Inhibition (mm in diameter)		
		Control	Stand*	Sample
1	*Bacillus subtilis*	-	16	16
2	*Escherichia coli*	-	16	14

3.7. Photocatalytic Studies

Fig. 7 shows the absorption spectra of MB at regular intervals throughout the whole degradation reaction with CG-Ag nanoparticles. The CG-Ag NPs were then kept under visible light radiation

at the start of the reaction with the fluid. 100 ml of methylene blue dye (MB) solution was swirled with 0.1g of generated CG-Ag nanoparticles at a concentration of 5 ppm in a conventional photocatalytic dye degradation procedure. Before being exposed to visible light, the stable aqueous dye solution was agitated for 50 minutes. Every 50 minutes, the experiment was repeated, and the UV-vis absorption spectra were recorded. The experiment lasted 150 minutes (one cycle), with the absorption spectrum collected every 50 minutes. In a probable graphic illustration of MB dye degradation, visible light irradiation produces an electron-hole (e^-/h^+) pair between the conduction band and the valence band of CG-Ag nanoparticles. MB dye is degraded into less harmful organic solutions or minerals by the active oxygen spices O_2, O_2•-, HOO•, and -OH [37, 38]. The pseudo-first-order model was used to investigate the reaction kinetics of MB dye using equation (1).

$$\ln (C_t/C_o) = kt \quad \ldots\ldots\ldots\ldots\ldots\ldots\ldots (1)$$

Where C_o is the initial dye concentration, C_t is the dye concentration after various irradiation durations, and 'k' is the photodegradation rate constant (min^{-1}) [39, 40]. Using an Ag catalyst generated from a solution ~pH 9 with a maximum degradation of about 84% is shown in Fig. 8, the stability of CG-Ag NPs against MB dye in a five-cycle process is examined. The CG-Ag NPS catalyst was recycled five times from the preceding patch of the experiment in this experiment. In this study, the reaction rate constant was calculated using the equation. A graph of $\ln(C_o/C)$ vs reaction time is shown in Fig. 9(a-b).

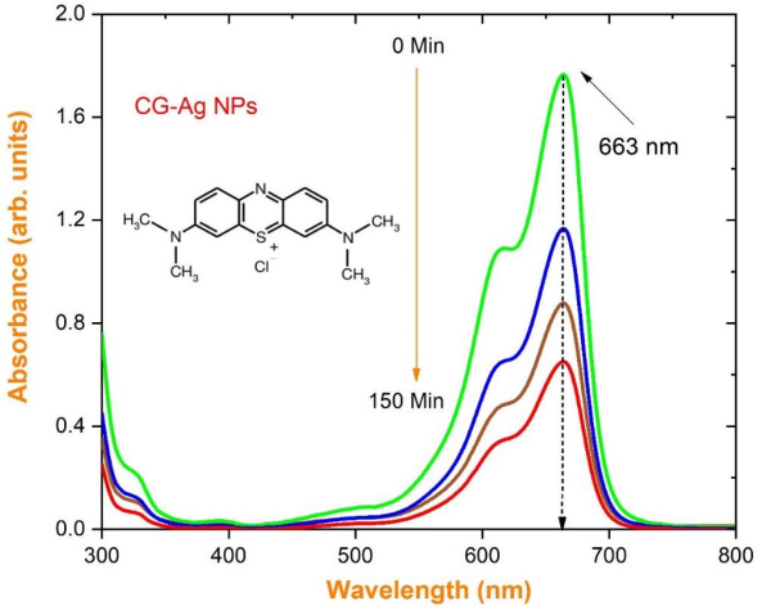

Fig. 7. Time dependent UV-vis absorption spectra of MB recorded in the existence of CG-Ag nanoparticles

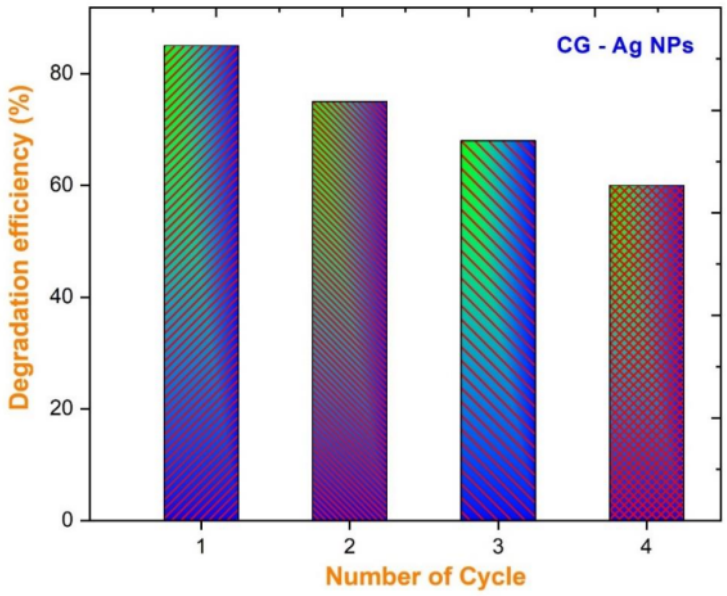

Fig. 8. Photocatalytic degradation efficiency bar diagram of CG-Ag nanoparticles.

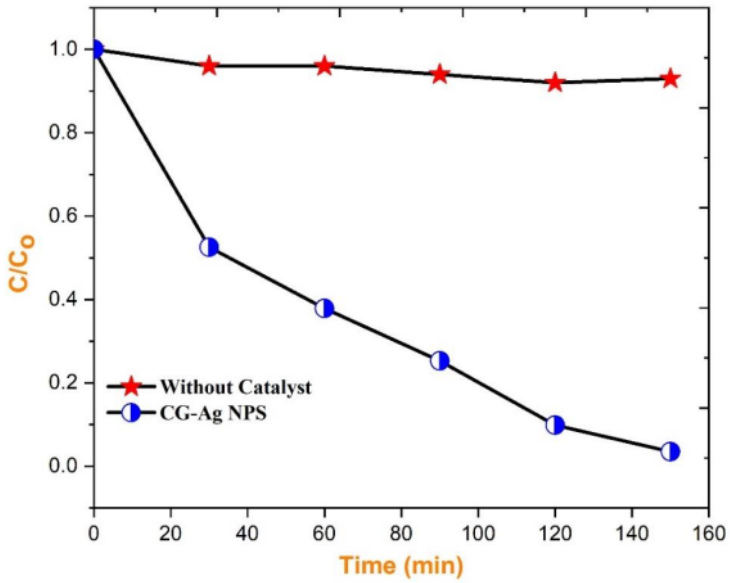

Fig. 9(a). Photocatalytic degradation efficiency of (a) C/C_o of CG-NPs

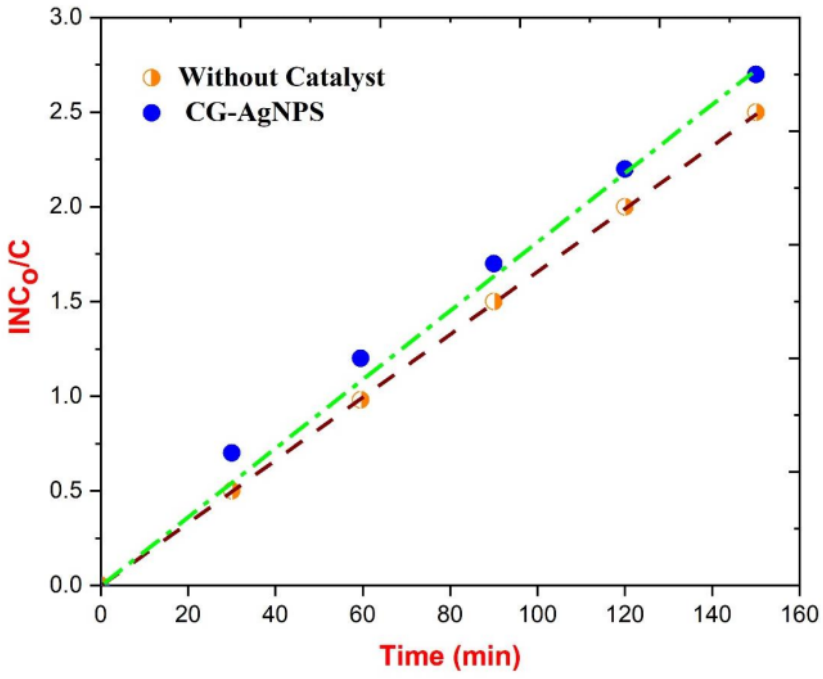

Fig. 9(b). Photocatalytic degradation efficiency of C_o/C of CG-NPs

From photocatalytic investigations of CG-AgNPs, we discovered that the rate constant for varying doses of MB dye is in the range of 0.0714 - 0.0592 min^{-1}. The photocatalytic efficiencies of the catalyst may be reduced because of the following possible cause. Continuous dye adsorption on the catalyst surface can deplete the active sites, reducing photocatalytic activity. Furthermore, incident light penetration to the catalyst surface can be reduced by the surface adsorbed dye, impacting the production of electron-hole pairs [41, 42]. This could explain why near the conclusion of the fifth cycle, the photodegradation efficiency of CG-Ag nanoparticles decreased. Fig. 10 depicts the reaction pathway that occurred during the photocatalytic activity of the CG-Ag nanoparticles photocatalyst under visible light.

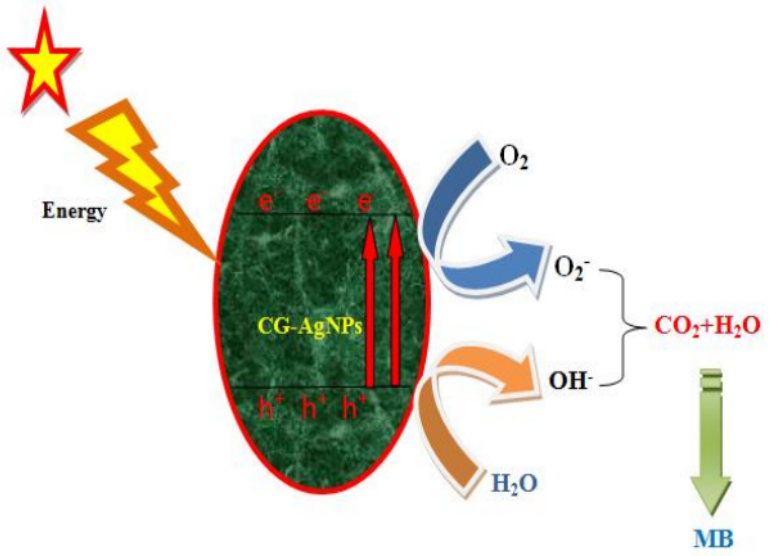

Fig. 10. Proposed photocatalytic reaction mechanism of CG-AgNPs photocatalyst

4. Conclusion

The present work is an attempt at plant-mediated nanoparticle synthesis and its characterization. The current study revealed that the extracts of the flower petals from *Couroupita guianensis* can synthesize Ag NPs fast, ecologically, economically, and in a renewable way. The produced silver nanoparticles were discovered to be crystalline with a face-centered cubic (FCC) shape. The typical crystallite size is 34 nanometers. The morphology showed that nanoparticles with an

average size of 32 nm have a trim dispersed flower shape, and the EDX validated the presence of elemental composition. The adequate reduction and stabilization of silver nanoparticles are due to phytochemicals, such as flavonoids, proteins, and phenolic compounds, which are produced in the extract of flower petals from Couroupita guianensis. Silver nanoparticles had remarkable antibacterial action against gram-positive bacteria when compared to Gram-negative bacteria (*Escherichia coli*) (*Bacillus subtilis*). The photocatalytic activity compared to CG-Ag NPs exhibited degradation of methylene blue dye. The degradation efficiency is found to be 90 % was witnessed on enhanced photocatalytic activity of CG-Ag NPs are suitable materials for environmental applications.

Declaration of Competing Interest

The authors declare that they have no known competing financial interests or personal relationships that could have appeared to influence the work reported in this paper.

Acknowledgements

The authors acknowledge management's efforts and express their gratitude. Also, authors thank the University of Douala, Cameroon for its support and encouragement.

References

AG

ORIGINALITY REPORT

14%	6%	12%	1%
SIMILARITY INDEX	INTERNET SOURCES	PUBLICATIONS	STUDENT PAPERS

PRIMARY SOURCES

1	N. Kumaresan, K. Ramamurthi, R. Ramesh Babu, K. Sethuraman, S. Moorthy Babu. "Hydrothermally grown ZnO nanoparticles for effective photocatalytic activity", Applied Surface Science, 2017 Publication	3%
2	Periasamy Anbu, Subash C.B. Gopinath, Hyun Shik Yun, Choul-Gyun Lee. "Temperature-dependent green biosynthesis and characterization of silver nanoparticles using balloon flower plants and their antibacterial potential", Journal of Molecular Structure, 2018 Publication	1%
3	link.springer.com Internet Source	1%
4	research.vit.ac.in Internet Source	1%
5	www.science.gov Internet Source	1%

6	www.researchgate.net Internet Source	1 %
7	www.scipress.com Internet Source	1 %
8	Majd said, yomen atassi, Mohammad Tally, Maissa Kattan, Lamia Kouba. "Antimicrobial Chitosan-G-poly(AMPS-Co-AA-Co-AM)/Ground Basalt Composite Hydrogel: Synthesis and Characterization", American Chemical Society (ACS), 2018 Publication	1 %
9	V. Ramalingam, R. Rajaram, C. PremKumar, P. Santhanam, P. Dhinesh, S. Vinothkumar, K. Kaleshkumar. " Biosynthesis of silver nanoparticles from deep sea bacterium JQ989348 for antimicrobial, antibiofilm, and cytotoxic activity ", Journal of Basic Microbiology, 2014 Publication	1 %
10	Liying Huang, Hui Xu, Yeping Li, Huaming Li, Xiaonong Cheng, Jixiang Xia, Yuanguo Xu, Guobin Cai. "Visible-light-induced WO3/g-C3N4 composites with enhanced photocatalytic activity", Dalton Transactions, 2013 Publication	<1 %

11	R. Vidhya, R. Gandhimathi, R. Karthikeyan, K. Neyvasagam. "Visible light driven enhancement in photodegradation of organic dyes using FexTi1-xO2 thin films", Materials Today: Proceedings, 2021 Publication	<1 %
12	Sivaji Sathiyaraj, Gunasekaran Suriyakala, Arumugam Dhanesh Gandhi, Ranganathan Babujanarthanam et al. "Chemical composition and mosquitocidal efficacy of panchagavya against Anopheles stephensi, Aedes aegypti and Culex quinquefasciatus", Journal of King Saud University - Science, 2022 Publication	<1 %
13	ijpsr.com Internet Source	<1 %
14	cees.kau.edu.sa Internet Source	<1 %
15	Farimehr Ghanizadeh Geraili, Seyed Mahmoud Reza Aghamiri, Marzieh Heidarieh. "Biosynthesis of silver nanoparticles using gamma irradiated of Iranian propolis extract", Research Square Platform LLC, 2022 Publication	<1 %
16	V. Perumal, A. Sabarinathan, M. Chandrasekar, M. Subash et al. "Hierarchical nanorods of graphene oxide decorated SnO2	<1 %

with high photocatalytic performance for energy conversion applications", Fuel, 2022
Publication

17	acris.aalto.fi Internet Source	<1 %
18	www.tandfonline.com Internet Source	<1 %
19	Ravishankar, T.N., K. Manjunatha, T. Ramakrishnappa, G. Nagaraju, Dhanith Kumar, S. Sarakar, B.S. Anandakumar, G.T. Chandrappa, Viswanath Reddy, and J. Dupont. "Comparison of the photocatalytic degradation of trypan blue by undoped and silver-doped zinc oxide nanoparticles", Materials Science in Semiconductor Processing, 2014. Publication	<1 %
20	Wenyue Zhang, Daquan Zhang, Xiaohui Li, Chunping Li, Lixin Gao. "Excellent performance of dodecyl dimethyl betaine and calcium gluconate as hybrid corrosion inhibitors for Al alloy in alkaline solution", Corrosion Science, 2022 Publication	<1 %
21	Fabrizio Ruggieri, Daniela Di Camillo, Livia Maccarone, Sandro Santucci, Luca Lozzi. "Electrospun Cu-, W- and Fe-doped TiO2 nanofibres for photocatalytic degradation of	<1 %

rhodamine 6G", Journal of Nanoparticle Research, 2013
Publication

Exclude quotes	Off	Exclude matches	Off
Exclude bibliography	Off		